

Water environment remote sensing atmospheric correction of geostationary ocean color imager data over turbid coastal waters in the Bohai Sea using artificial neural networks

Liqiao Tian¹, Qun Zeng^{2,*}, Xiaojuan Tian², Jian Li¹, Zheng Wang^{3,4} and Wenbo Li⁵

¹State Key Laboratory of Information Engineering in Surveying, Mapping and Remote Sensing, Wuhan University, Wuhan, Hubei, China

²School of Urban and Environment Science, Huazhong Normal University, Wuhan 430079, Hubei, China

³Nanjing University, Nanjing, Jiangsu Province 210023, China

⁴State Key Laboratory of Satellite Ocean Environment Dynamics, Second Institute of Oceanography, State Oceanic Administration, 36 Bochubeilu, Hangzhou 310012, China

⁵Institute of Intelligent Machines, Chinese Academy of Sciences, Hefei 230031, China

The Geostationary Ocean Color Imager (GOCI) can produce good ocean colour products in the open sea. However, an atmospheric correction problem continues to occur for turbid coastal water environment monitoring. In this communication, a regional atmospheric correction method based on an artificial neural network (ANN) model has been proposed. The ANN model was built according to differences in the spatial and radiometric characteristics between the Medium Resolution Imaging Spectrometer (MERIS) and GOCI, with 3000 pixels of the top-of-atmosphere (TOA) reflectance of seven GOCI images from 2011 to 2012 above turbid water used as the inputs and coinciding validated remote-sensing reflectance (Rrs) of MERIS¹ used as the outputs. Subsequently, the water-leaving reflectance of GOCI in turbid coastal water areas of the Bohai Sea was derived. Compared with the products produced by the standard GOCI Data Processing System (GDPS Version 1.3), the Rrs retrieved according to the proposed method showed a significant improvement in spatial pattern. Although the ANN model displayed a degree of difficulty in representing high water-leaving reflectance values, a comparison with three *in situ* measurements collected on 11 November 2011 in the study area showed encouraging results. The results suggest that the ANN method can be used for atmospheric correction process in turbid waters without requiring numerous *in situ* measurements.

Keywords: Artificial neural network, atmospheric correction, ocean color imager, remote sensing, turbid coastal waters.

THE first geostationary ocean color satellite sensor, the Geostationary Ocean Color Imager (GOCI), was success-

fully launched in June 2010 on-board the South Korean Communication, Ocean, and Meteorological Satellite (COMS)². It has six visible bands centred at 412, 443, 490, 555, 660 and 680 nm, and two near-infrared (NIR) bands at 745 and 865 nm with eight daytime measurements from 9:00 to 16:00 local time³. GOCI was developed to monitor marine environments and realize real-time rapid data acquisition⁴. In addition, over two-thirds of the coastal waters in China could be covered by the hourly GOCI images, which greatly benefits remote sensing capabilities for water environments in China.

Generally, the total signals at satellite altitudes are comprised of atmospheric path radiance and water-leaving information^{5,6}. The latter plays an important role in the ocean colour remote sensing application to retrieve bio-optical properties; thus, atmospheric correction is a key procedure before the water constituents can be inverted^{7,8}. For case-I water, the atmospheric correction algorithm proposed by Gordon and Wang⁷ is effective. However, it tends to give unreasonable aerosol scattering radiance and water-leaving results in turbid coastal waters because of the invalid black pixel assumption in the NIR spectrum⁶.

To avoid the atmospheric correction failure problem in turbid waters, a novel improved GOCI default algorithm in GDPS version 1.3 iteratively restores water-leaving reflectance at 745 and 865 nm bands from an empirical relationship model that is constructed for water-leaving reflectance at the red and NIR bands, by assuming that turbid water reflectance relationships of the red and NIR bands are dominated by inorganic particles. To build the empirical relationship model, satellite-derived water reflectance data by the nearby non-turbid atmospheric correction were used⁶. Unfortunately, the current GOCI atmospheric correction algorithm included in the GDPS version 1.3, similar to the iterative scheme proposed by Wang *et al.*⁹, does not still work accurately for extremely turbid waters¹⁰. In addition, turbid water pixels are often masked due to cloud; so the GDPS version 1.3 still cannot give reasonable spatial pattern in the coastal turbid water area.

Artificial neural network (ANN) is a widely used information processing paradigm to fit nonlinear transfer functions¹¹. During the past decades, several studies have been conducted with ANN to remove the atmospheric influence of satellite measurements. Schröder *et al.*¹² proposed an ANN-based method for multiple scattering and absorbing aerosols correction to retrieve the water-leaving reflectance and chlorophyll concentration over open sea waters. The atmospherically corrected remote sensing reflectance (Rrs), aerosol optical depth (AOD) and bio-optical parameters concentration from total or 'Rayleigh corrected' top-of-the-atmosphere (TOA) reflectance were also retrieved from several separate ANNs according to the radiative transfer (RT) models by considering various atmospheric and oceanic conditions¹³⁻¹⁵.

*For correspondence. (e-mail: zq@mail.cnu.edu.cn)

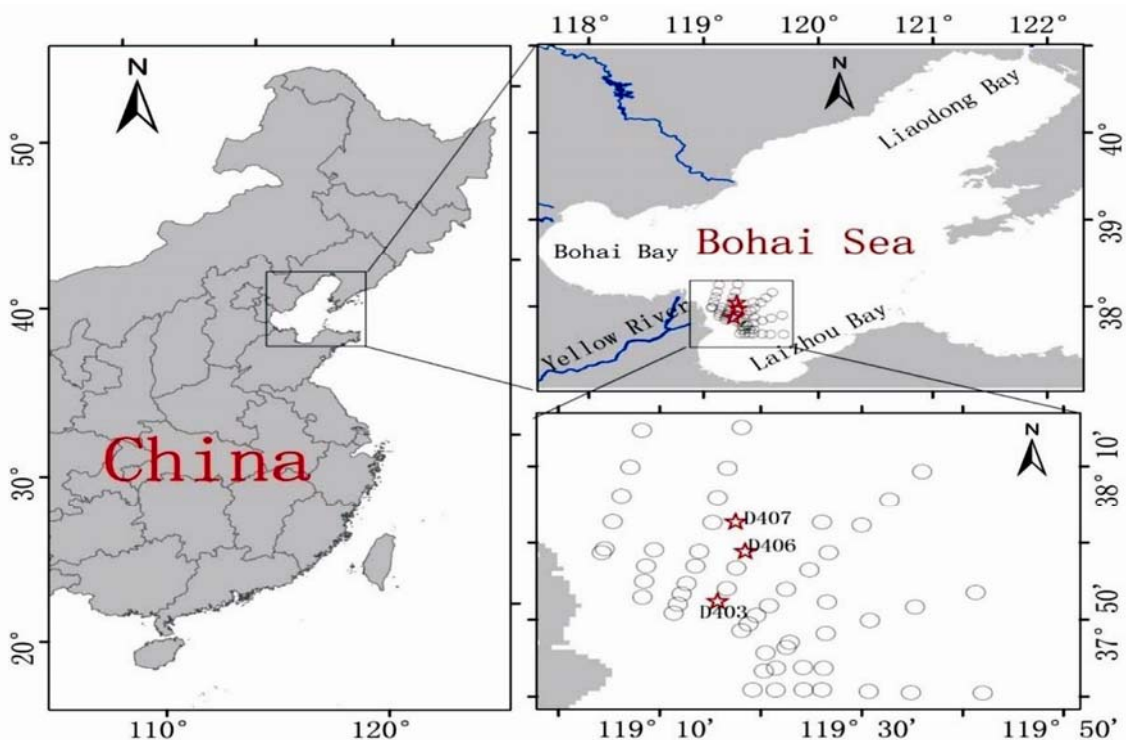


Figure 1. Geographical locations of the Bohai Sea and sample stations in November and December 2011. The hollow black circles represent mobile stations and the red stars represent stationary stations.

Table 1. Description of the 2011 and 2012 ocean color satellite datasets. For each date, the GOCI data are those recorded at noon (local time, i.e. 03:16 UTC), while Δt (\pm hh : mm) is the time difference with the MERIS satellite data

Year	Date	GOCI (UTC in hh : mm)	MERIS (Δt in hh : mm)
2011	3 April	03 : 16	-00 : 27
	3 May	03 : 16	-00 : 27
	13 June	03 : 16	-00 : 25
2012	27 February	03 : 16	-00 : 30
	9 March	03 : 16	-00 : 27
	31 March	03 : 16	-00 : 14
	5 April	03 : 16	-00 : 23

In addition, a combination of ANN techniques and variational inversion methods was also proposed to correct for the problem of absorbing aerosols^{16,17}.

In this communication we propose an ANN atmospheric correction scheme to process GOCI images in turbid coastal waters. Comparisons with GDPS-derived results and simultaneous *in situ* measurements in the turbid water area of the Bohai Sea showed that the proposed atmospheric correction method is valid.

The Bohai Sea is a semi-enclosed, large, turbid and shallow sea (117°38'–122°12'E, 37°10'–40°51'N). It is usually divided into four parts, i.e., Liaodong Bay, Bohai Bay, Laizhou Bay and Central Bohai Sea (Figure 1). The

mean water depth in the Bohai Sea is approximately 18 m. The Bohai Strait is the link between the Bohai Sea and the Yellow Sea, where the greatest water depth is about 80 m. More than 17 rivers bring a great quantity of suspended sediments into the Bohai Sea¹⁸. Thus, the majority of the Bohai Sea is case-II water, because suspended matter is a non-ignorable contributor of water optical characteristics¹⁹.

GOCI performs hourly measurement during the day and has the ability to provide optional data for monitoring highly dynamic aquatic environments³.

The GOCI level-1 B (L1B) data products were downloaded from the following website: http://engkoscnw.intnaray.net/kosc_eng/GOCI_download/SatelliteData.html. The Medium Resolution Imaging Spectrometer (MERIS) was launched on-board the Envisat satellite in 2002 by the European Space Agency (ESA) and retired on 8 April 2012. MERIS L2 data products were collected from ESA for the DRAGON project (<http://earth.esa.int/dragon/>) and water-leaving reflectance results for case-2 waters based on the 'bright-pixel' atmospheric correction model were validated in the Bohai Sea and its adjacent turbid coastal waters^{1,20}. In order to overcome the time limitations, seven synchronous GOCI and MERIS images without cloud, haze and Sun glint contamination during different seasons in 2011 and 2012 were processed to build the ANN model used to atmospherically correct GOCI data (Table 1). All the MERIS products were

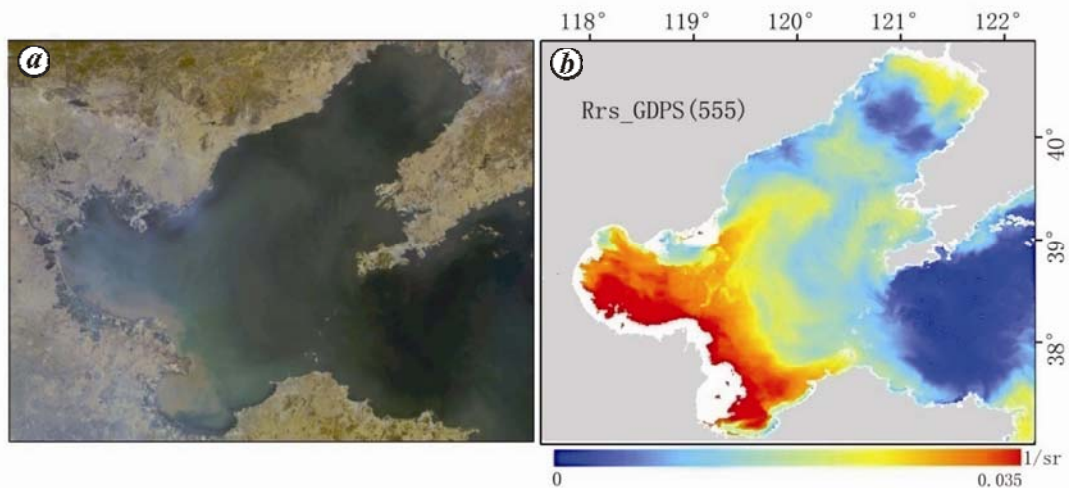


Figure 2. (a) GOCI image RGB display (R, G, B = bands 6, 4, 1) and (b) its derived remote sensing reflectance (R_{rs} , R_r^{-1}) at 555 nm using GDPS v1.3 software on 3 April 2011 at noon local time.

Table 2. GOCI spectral bands and corresponding wavebands for MERIS

GOCI			MERIS				
Band	λ (nm)	$\Delta\lambda$ (nm)	Band	λ (nm)	$\Delta\lambda$ (nm)	Match-ups	R^2
B1	412	20	B1	412.5	10	28930	0.908936
B2	443	20	B2	442.5	10	32555	0.926560
B3	490	20	B3	490	10	30072	0.942771
B4	555	20	B5	560	10	14421	0.947873
B5	660	20	B7	665	10	14862	0.948877
B6	680	10	B8	681.25	7.5	16795	0.927346

geo-referenced and resampled to 500 m, applying the nearest-neighbour approach to reference GOCI images (longitude–latitude projection, World Geodetic System (WGS)-84). The root-mean-square error (RMSE) is less than half a pixel.

A field campaign was conducted in the Bohai Sea in November and December 2011 (Figure 1). During the survey, about 68 reflectance measurements were taken by an SVC (Spectra Vista Corporation, Inc.) HR-1024 field-portable spectroradiometer from 350 to 2500 nm in 4 nm increments, according to the NASA-suggested protocols for optical measurements. That is, a viewing direction of 40° from the nadir and 135° from the Sun to minimize the effects of Sun glint and non-uniform sky radiance and to avoid instrument shading problems^{21,22}. However, due to cloudy weather conditions, just three simultaneous *in situ* spectral observations in the GDPS-failure area (Figure 2) on 11 December 2014 could be selected for validation.

In case-I waters, the water-leaving radiance at 745 and 865 nm ($L_w(745)$ and $L_w(865)$) is assumed zero, and the aerosol radiance ($L_{ma}(\lambda_i)$) at NIR bands can be easily obtained and extrapolated to the visible spectrum^{7,23}. The default atmospheric correction method embedded in GDPS version 1.3 is partially modified for the atmos-

pheric multiple scattering influence corrections in case-2 water based on the optimized aerosol model and solar angle information. However, this method tends to produce no valid results in turbid coastal waters.

The R_{rs} on 3 April 2011 at noon local time was retrieved by GDPS version 1.3 and displayed in (Figure 2). Obviously, turbid coastal waters near the Yellow River in the Bohai Sea are covered by invalid values, and atmospheric corrections over these areas should be the focus. Two critical issues must be addressed before the proposed method can be used to remove the atmospheric influence of GOCI: cross-sensor agreement and the ANN model.

Despite differences in the spatial and radiometric properties between MERIS and GOCI, similarities in their band arrangements indicate the possibility of building a network using MERIS data Table 2. However, correcting GOCI images using MERIS information based on the ANN model is difficult because of mismatches of the sensors in (1) band settings, (2) solar and satellite geometry, (3) signal-to-noise ratio (SNR) and (4) observation time. Although the differences in their overpass time within ~ 1 h may have no great changes either in the atmospheric or aquatic environment, other issues must be

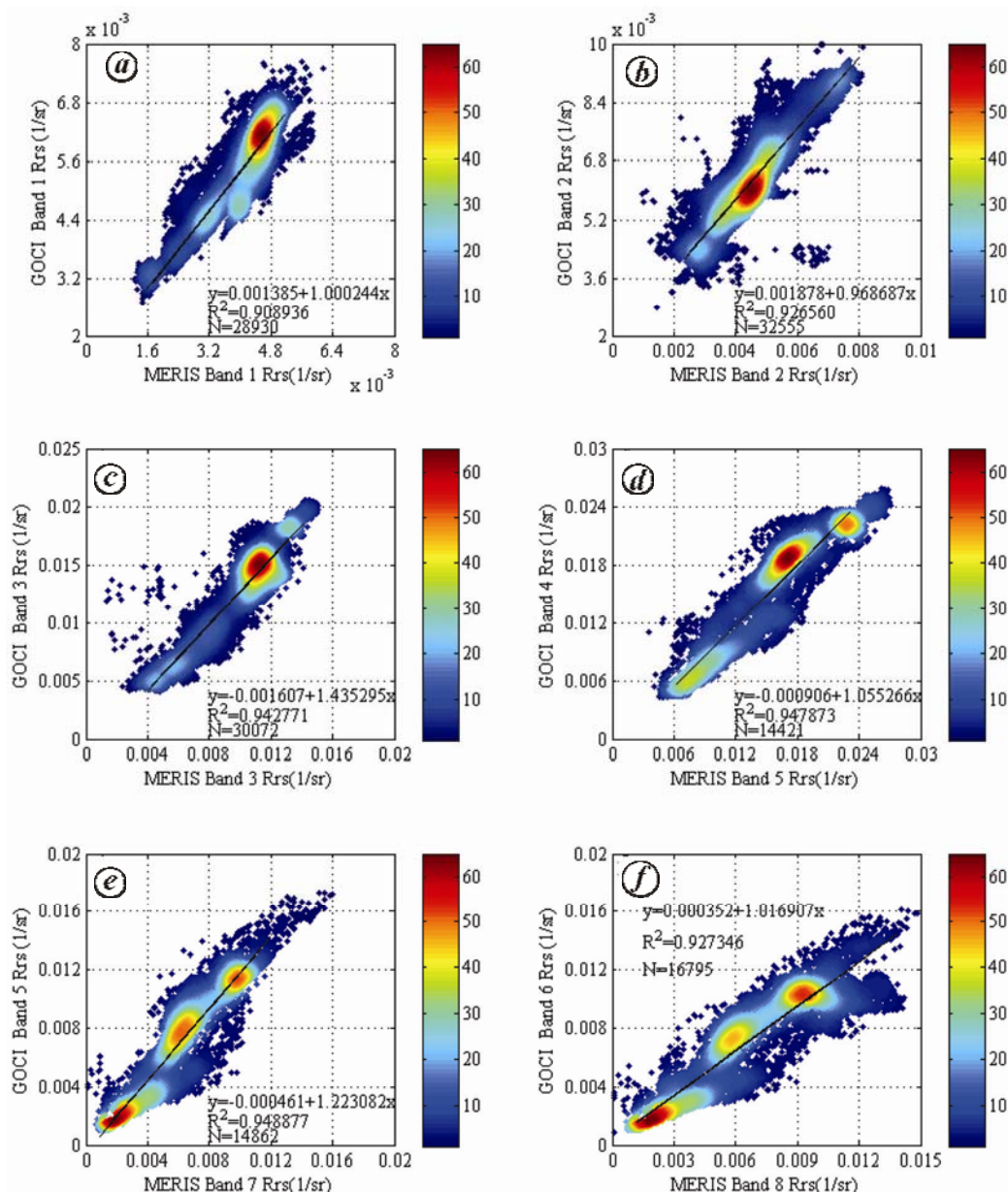


Figure 3. Scatter plots showing match-ups of MERIS and GOCI remote sensing reflectance ($Rrs(\lambda_i)$) from clear water at the (a) 412, (b) 443, (c) 490, (d) 555, (e) 660, and (f) 680 nm bands.

adequately addressed before MERIS data can be used as the target outputs of GOCI data in turbid waters. Thus, an approach must be developed to overcome these obstacles by increasing the consistency between MERIS data and GOCI data, and subsequently assessing the inherent differences of each data source.

In this study, concurrent (within ~1 h) and collocated GOCI and MERIS Rrs measurements, hereby referred to as ‘match-ups’ (n), over clear water areas were picked up and corrected by linear regression for the corresponding six visible bands. Outliers caused by mixed pixels in the samples were discarded before the regression processing based on an iterative procedure proposed in a previous

study²⁴. Positive linear trends were used to describe the relationships between the GOCI and MERIS data at each visible band (Table 2 and Figure 3). In the next step, MERIS data were converted by the function determined by the regression analysis (Figure 3) and used to retrieve the target Rrs of GOCI for turbid waters.

We now briefly describe the multilayer perceptron and its application in nonlinear regression, and then illustrate the mathematical foundation employed to optimize the parameters of nonlinear functions.

An ANN is a parallel-distributed processor that resembles the human brain²⁵. It has a natural propensity for storing experiential knowledge and making it available

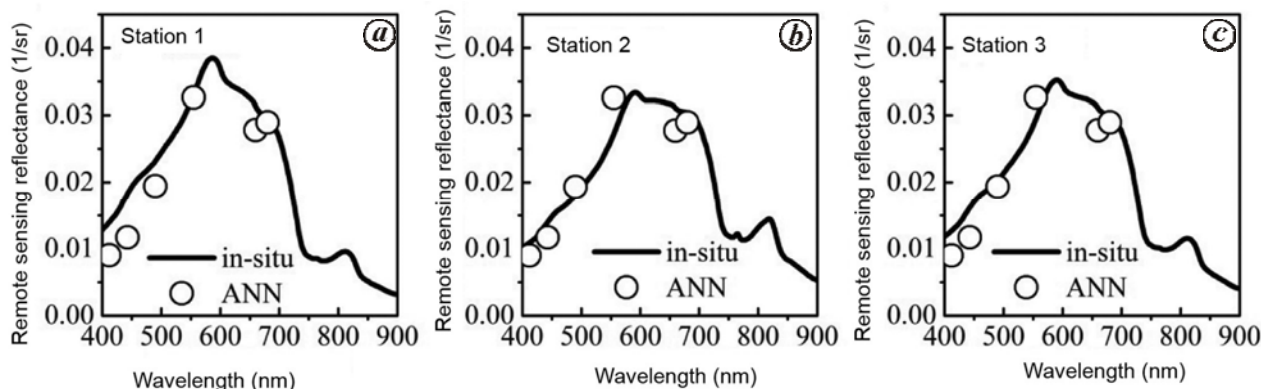


Figure 6. Comparison of the remote sensing reflectance (Sr^{-1}) at various visible bands from the ANN model-based atmospheric correction method with three *in situ* measurements.

for use. The task of neurons is to perform non-linear function approximations. The neural network used in the present experiment is a multilayer, feed-forward-type model. These networks have one input layer, one output layer and some hidden layers between them. A theoretical background is not available for the number of hidden layers (i.e. neurons) that must be considered; so we should confirm the optimal network structure for this problem through trial and error²⁶.

In this experiment, optimal outputs are obtained when we use a network with ten hidden layers. Each input node represents a band of GOCI imagery. The ten nodes in the ‘hidden’ layer receive the values from the input layer to perform the summation and activation functions. Then the target values of the output layer of the network would compare the output information of the hidden layer based on the computation. The result of the output layer is the information on the bio-optical properties concerned, as seen in eq. (1)

$$\text{Output} = \left(\alpha g \sum_{k=1}^j \omega_k z_k + \beta \right), \quad (1)$$

where ω_k is the weight of neurons, β the bias of the output layer and j is the number of nodes which are in the hidden layer. The scaled factor α of the output is determined in the training processing. It has been shown that a neural network with one hidden layer can realize any function regardless of complexity based on the Kolmogorov’s representation theorem²⁷. So ANN could be used to retrieve water-leaving reflectance from the GOCI TOA radiance.

The task of the network is to calculate the Rrs of GOCI in the visible bands in turbid waters using Matlab version R2011a (MathWorks). Using the 3000TOA reflectance of GOCI from turbid water as the input and the coinciding converted Rrs of MERIS (bands 1, 2, 3, 5, 7, 8) as the output, an ANN was trained and established to simulate

the water-leaving reflectance of GOCI in turbid water areas (Figure 4).

To assess the proposed method, we applied the ANN atmospheric correction model to several GOCI scenes over the Bohai Sea and its adjacent turbid coastal waters. Figure 5 displays the atmospherically corrected results of GOCI for the six visible bands in the study area on 3 April 2011 at noon local time. Compared with the outputs displayed in Figure 2 b, the results in Figure 5 are significantly improved, especially in the turbid coastal water areas near the Yellow River that were masked in GDPS version 1.3.

In addition, all the ANN atmospheric correction results were validated using the three synchronous *in situ* data of the water-leaving reflectance on 11 December 2014. Because of the high time resolution of GOCI (eight images during the day), there is only approximately 1–3 min difference between the GOCI and *in situ* observations.

Figure 6 compares the ANN-based water-leaving reflectance and *in situ* measurements at each available station. Overall, the GOCI ANN-based Rrs (λ) at 412, 443, 490, 555, 660 and 680 nm generally matches the values and spectral shapes reasonably well with the simultaneous *in situ* collections in the turbid water region (Figure 6). Figure 6 also shows that the visible bands are highly consistent. However, the error is slightly higher in the bands at central wavelengths of 412, 443, 660 and 680 nm than those of 490 and 550 nm between the corrected results and *in situ* data, which may have been caused by the higher error of bands 1, 2, 7 and 8 in the corresponding MERIS remote sensing reflectance products¹. In addition, the ANN model also has some errors. Therefore, additional attention should be focused on improving the accuracy of the corrected results at these bands over higher turbid water areas in the future.

An atmospheric correction method based on the ANN model was proposed for GOCI data corresponding to Bohai Sea turbid coastal waters based on the validated and cross-calibrated MERIS water-leaving reflectance

products. Compared with the GDPS-derived product (version 1.3), the proposed scheme can avoid atmospheric correction failures and provide reasonable spatial patterns for GOCI data in turbid coastal water. The results also show that the satellite-corrected reflectance is comparable with the three simultaneous *in situ* data records. The results showed that ANNs are effective at removing atmosphere influence over turbid waters. The model and outputs discussed here provide an effective option for the atmospheric correction processing of GOCI or other satellite images without SWIR bands in turbid water regions. Our results will be helpful for monitoring water environments of case-II waters.

Although the ANN-based approach in the present study showed atmospheric correction spatial pattern improvements and good agreement with *in situ* data in turbid coastal waters, more improvement and validation are needed in the future.

1. Cui, T., Zhang, J., Groom, S., Sun, L., Smyth, T. and Sathyendranath, S., Validation of MERIS ocean-color products in the Bohai Sea: a case study for turbid coastal waters. *Remote Sensing Environ.*, 2010, **114**, 2326–2336.
2. Neukermans, G., Ruddick, K. G. and Greenwood, N., Diurnal variability of turbidity and light attenuation in the southern North Sea from the SEVIRI geostationary sensor. *Remote Sensing Environ.*, 2012, **124**, 564–580.
3. Hu, C., Feng, L. and Lee, Z., Evaluation of GOCI sensitivity for at-sensor radiance and GDPS-retrieved chlorophyll-*a* products. *Ocean Sci. J.*, 2012, **47**, 279–285.
4. Ryu, J., Choi, J., Eom, J. and Ahn, J., Temporal variation in Korean coastal waters using Geostationary Ocean Color Imager. *J. Coastal Res.*, SI64, 2011, 1731–1735.
5. Gordon, H. R., Atmospheric correction of ocean color imagery in the earth observing system era. *J. Geophys. Res. Atmos. (1984–2012)*, 1997, **102**, 17081–17106.
6. Hu, C., Carder, K. L. and Muller-Karger, F. E., Atmospheric correction of SeaWiFS imagery over turbid coastal waters: a practical method. *Remote Sensing Environ.*, 2000, **74**, 195–206.
7. Gordon, H. R. and Wang, M., Retrieval of water-leaving radiance and aerosol optical thickness over the oceans with SeaWiFS: A preliminary algorithm. *Appl. Opt.*, 1994, **33**, 443–452.
8. Gordon, H. R. and Franz, B. A., Remote sensing of ocean color: assessment of the water-leaving radiance bidirectional effects on the atmospheric diffuse transmittance for SeaWiFS and MODIS intercomparisons. *Remote Sensing Environ.*, 2008, **112**, 2677–2685.
9. Wang, M., Shi, W. and Jiang, L., Atmospheric correction using near-infrared bands for satellite ocean color data processing in the turbid western Pacific region. *Opt. Express*, 2012, **20**, 741–753.
10. Wang, M., Ahn, J.-H., Jiang, L., Shi, W., Son, S., Park, Y.-J. and Ryu, J.-H., Ocean color products from the Korean Geostationary Ocean Color Imager (GOCI). *Opt. Express*, 2013, **21**, 3835–3849.
11. Gross, L., Thiria, S. and Frouin, R., Applying artificial neural network methodology to ocean color remote sensing. *Ecol. Model.*, 1999, **120**, 237–246.
12. Schröder, T., Fischer, J., Schaale, M. and Fell, F. (eds), Artificial-neural-network-based atmospheric correction algorithm: application to MERIS data. In Third International Asia-Pacific Environmental Remote Sensing of the Atmosphere, Ocean, Environment, and Space, International Society for Optics and Photonics, pp. 124–132.
13. Schröder, T., Behnert, I., Schaale, M., Fischer, J. and Doerffer, R., Atmospheric correction algorithm for MERIS above case-2 waters. *Int. J. Remote Sensing*, 2007, **28**, 1469–1486.
14. Schiller, H. and Doerffer, R., Neural network for emulation of an inverse model operational derivation of case ii water properties from MERIS data. *Int. J. Remote Sensing*, 1999, **20**, 1735–1746.
15. Schröder, T., Schaale, M. and Fischer, J., Retrieval of atmospheric and oceanic properties from MERIS measurements: a new case-2 water processor for beam. *Int. J. Remote Sensing*, 2007, **28**, 5627–5632.
16. Brajard, J., Jamet, C., Moulin, C. and Thiria, S., Use of a neuro-variational inversion for retrieving oceanic and atmospheric constituents from satellite ocean colour sensor: application to absorbing aerosols. *Neural Networks: Off. J. Int. Neural Network Soc.*, 2006, **19**, 178–185.
17. Doerffer, R., Alternative atmospheric correction procedure for case 2 water remote sensing using MERIS. *MERIS ATBD*, 2011, **2**.
18. Chen, J., Quan, W., Wen, Z. and Cui, T., An improved three-band semi-analytical algorithm for estimating chlorophyll-*a* concentration in highly turbid coastal waters: a case study of the Yellow River Estuary, China. *Environ. Earth Sci.*, 2013, **69**, 2709–2719.
19. Chen, J. and Quan, W., An improved algorithm for retrieving chlorophyll-*a* from the Yellow River estuary using MODIS imagery. *Environ. Monit. Assess.*, 2013, **185**, 2243–2255.
20. Moore, G. F., Aiken, J. and Lavender, S. J., The atmospheric correction of water colour and the quantitative retrieval of suspended particulate matter in case ii waters: application to MERIS. *Int. J. Remote Sensing*, 1999, **20**, 1713–1733.
21. Lee, Z., Carder, K., Steward, R., Peacock, T., Davis, C. and Mueller, J. (eds), Protocols for measurement of remote-sensing reflectance from clear to turbid waters. In SeaWiFS Workshop, Halifax, Canada.
22. Mobley, C. D., Estimation of the remote-sensing reflectance from above-surface measurements. *Appl. Opt.*, 1999, **38**, 7442–7455.
23. Gordon, H. R. and Voss, K. J., MODIS normalized water-leaving radiance algorithm theoretical basis document. NASA Technical Report Series, NAS5-31363, 1999.
24. Li, X., Chen, X., Zhao, Y., Xu, J., Chen, F. and Li, H., Automatic inter calibration of night-time light imagery using robust regression. *Remote Sensing Lett.*, 2012, **4**, 45–54.
25. Hykin, S., *Neural Networks: A Comprehensive Foundation*, Prentice-Hall, New Jersey, 1999.
26. Beale, R. and Jackson, T., *Neural Computing – An Introduction*, CRC Press, 2010.
27. Landau, S. and Everitt, B., *A Handbook of Statistical Analyses using SPSS*, Chapman & Hall/CRC Boca Raton, FL, 2004.

ACKNOWLEDGEMENTS. This work was supported by the National Natural Science Foundation of China (nos. 41571344, 41406205), the Open Research Fund of the Key Laboratory of Space Ocean Remote Sensing and Application, State Oceanic Administration of the People's Republic of China (No. 201502003), the Open Research Fund of State Key Laboratory of Simulation and Regulation of Water Cycle in River Basin, China Institute of Water Resources and Hydropower Research (IWRH-SKL-201514). We thank Dr Tingwei Cui and the Korea Ocean Satellite Center for GOCI dataset, MERIS products and the field measurements support.

Received 18 August 2015; revised accepted 7 November 2015

doi: 10.18520/cs/v110/i6/1079-1085